Received: 29 May 2025 | Revised: 19 February 2026 | Accepted: 10 March 2026

DOI: 10.1002/qj.70187

Quarterly Journal of the Royal Meteorological Society RMetS

RESEARCH ARTICLE

Diagnosing the 11-year solar cycle's influence on the East Atlantic pattern

Stergios Misios[1] | **Paula L. M. Gonzalez**[2,3] | **Lesley J. Gray**[2,4] | **Scott Osprey**[2,4] | **Hedi Ma**[5]

[1]Research Centre for Atmospheric Physics and Climatology, Academy of Athens, Athens, Greece

[2]National Centre for Atmospheric Science, Leeds, UK

[3]University of Reading, Reading, UK

[4]Department of Physics, Oxford University, Oxford, UK

[5]Hubei Key Laboratory for Heavy Rain Monitoring and Warning Research, Institute of Heavy Rain, China Meteorological Administration, Wuhan, China

Correspondence
Stergios Misios, Research Centre for Atmospheric Physics and Climatology, Academy of Athens, Athens, Greece.
Email: smisios@academyofathens.gr

Funding information
Natural Environment Research Council, Grant/Award Numbers: NE/V013130/1, NE/R000034/1; CANARI programme; National Centre for Atmospheric Science; Global Challenges Research Fund, Grant/Award Number: NE/R000034/1; NCAS National Capability Programme ACREW, Grant/Award Number: NE/R000034/1; Hellenic Foundation for Research and Innovation, Grant/Award Number: 3995

Abstract

The North Atlantic sector has been identified as a region where the 11-year solar cycle has small but potentially non-negligible impacts on winter climate, but a debate persists about the robustness of such impacts. This work explores the signatures of the 11-year solar cycle over the North Atlantic in the ERA5 and 20th Century Reanalysis datasets. The results confirm previous studies with a robust positive boreal winter response in mean-sea-level pressure (mslp) in the region of the Azores at lags of three years after solar maximum. The spatial evolution of the response is examined in detail by first decomposing the mslp time series into the dominant modes of North Atlantic winter mslp variability, including the North Atlantic Oscillation (NAO), the East Atlantic (EA) and the Scandinavian patterns, before performing a multilinear regression analysis. We find that the maximum 11-year solar response in the December–January–February (DJF) average does not project directly onto the NAO. However, when the early/late-winter responses are examined separately, a statistically significant NAO response is seen in late winter (January–February) at lag 0–1 years and a statistically significant NAO response is also seen at lag +3 years in early winter (November–December). These results are consistent with predicted responses from previously proposed top-down influences from the stratosphere in late winter followed by the re-emergence of a signal from underlying sea surface temperatures in early winter. However, the NAO response is not the primary contributor to the total DJF response at lag +3 years. A previously unidentified solar-cycle response in the EA pattern is found in late winter at lag +3 years with larger amplitude than the NAO response. The evolution of the DJF mslp response over the Azores region can thus be understood as a summation of the NAO and EA patterns at lag +3 years.

KEYWORDS

empirical orthogonal functions, North Atlantic Oscillation, solar cycle

1 | INTRODUCTION

The 11-year solar cycle (SC) is characterised by a quasi-periodic oscillation in solar irradiance received at the top of the atmosphere (Lean & Rind, 2009). Variations in total solar irradiance (TSI) are dominated by energy in the visible part of the spectrum that can penetrate the atmosphere and reach the Earth's surface. The resulting impacts arrive via the so-called 'bottom-up' pathway, through its direct influence on sea surface temperatures (SSTs) which can then indirectly influence patterns of weather and climate from below (Gray *et al.*, 2010; Meehl *et al.*, 2009; Misios & Schmidt, 2012). TSI variations over the 11-year SC are associated with a global-average SST response of approximately 0.1 K (White *et al.*, 2003). As a result of thermal inertia of the oceans the peak global SST response is generally found to lag the peak 11-year solar activity by approximately 1–2 years (Misios *et al.*, 2016; White *et al.*, 1997).

In addition, several indirect 'top-down' mechanisms have been proposed, for example through variations in the ultraviolet part of the solar radiation spectrum (Chiodo *et al.*, 2012; Gray *et al.*, 2010; Haigh, 2001; Ineson *et al.*, 2011; Kodera & Kuroda, 2002; Thieblemont *et al.*, 2015) and/or through variations in energetic particles (Maliniemi *et al.*, 2019; Seppälä & Clilverd, 2014). Their effects can penetrate to the upper stratosphere and be amplified by ozone responses (Haigh, 2001; Hood & Soukharev, 2012). Previous work highlighted that the top-down influences at midlatitudes act mainly in winter and extend their influence downwards to the surface via wave–mean flow interaction, so that relatively small variations in the equatorial upper stratosphere of only 1–2 K can be amplified and transferred to the surface at mid- and high latitudes (Gray *et al.*, 2010; Kodera & Kuroda, 2002).

There are also several potential interactions of the bottom-up and top-down pathways. The bottom-up pathway influences equatorial SSTs, deep convection (together with associated precipitation rates) and vertical velocities associated with the Hadley and Walker circulations (Misios *et al.*, 2019). Associated influences on El Nino/La Nina events (Meehl *et al.*, 2009; Roy & Haigh, 2010; Tung & Zhou, 2010) and/or the large-scale atmospheric Rossby waves that are generated at equatorial latitudes and propagate into midlatitudes (Scaife *et al.*, 2017) could also influence the midlatitude circulation. Other studies have found that the synergistic effects of bottom-up and top-down influences in the summer monsoon region amplify the monsoon's response to the SC, affecting precipitation patterns (e.g., Zhao *et al.*, 2025). The quasi-biennial oscillation (QBO) is also affected by changes in vertically-propagating equatorial waves and the strength of equatorial upwelling (García-Franco *et al.*, 2022). Interaction of the SC and the QBO (Labitzke & van Loon, 2000) could then influence wave propagation in the winter stratosphere and thus impact the surface via the top-down mechanism. In addition, subtropical lower-stratosphere temperature anomalies associated with SC influences on the Hadley/Walker/QBO circulations could influence synoptic-scale eddies in the upper troposphere (Haigh & Blackburn, 2006) with accompanying impacts at the surface.

The 11-year SC has been previously linked to impacts in North Atlantic (NA) winter surface climate (Gray *et al.*, 2013; Lockwood *et al.*, 2010; Woollings *et al.*, 2010). Observations and model simulations provide evidence for a possible 'top-down' forcing in the region, via a modulation of the stratospheric polar vortex and a downward propagation of wind anomalies that influence annual modes of variability in the troposphere (e.g., Kodera & Kuroda, 2002; Kuroda *et al.*, 2022). However, this region is influenced by many different forcing and feedback processes. Seasonal-to-interannual atmospheric variability in the NA sector is dominated by the North Atlantic Oscillation (NAO), particularly during boreal winter (Hurrell & van Loon, 1997) and is also influenced by other global modes of variability including, for example, the Pacific–North American wave-train, the El Nino–Southern Oscillation and variability of the stratospheric polar vortex. The region also shows strong susceptibility to the influence of forced variability and feedbacks such as anthropogenic aerosols (e.g., Bellouin *et al.*, 2020), volcanic activity (e.g., Swingedouw *et al.*, 2017) and arctic amplification (e.g., Barnes & Polvani, 2015). Interactions between these natural and forced sources of variability add to the climatic complexity of the region (Dimdore-Miles *et al.*, 2021; Klavans *et al.*, 2022; Ottera *et al.*, 2010) so that solar signal detection is particularly challenging.

Detection and attribution of the surface solar response in the NA DJF (December–January–February) has also been complicated by the fact that the maximum observed response is lagged by several years. This was first identified by Gray *et al.* (2013) using the historical gridded HadSLP and HadISST observational datasets that span approximately 150 years. They identified a mean-sea-level pressure (mslp) response that amplified and evolved for several years following the maximum in solar forcing (S_{max}). The largest (positive) statistically significant response in DJF mslp of up to 3 hPa was found in the region of the southern node of the NAO near the Azores, with a lag of 3–4 years, that is, approximately one quarter of a SC. This is a substantial signal against a background standard deviation of around 6–7 hPa for DJF mslp (see fig. 1 of Gray *et al.* (2016)). A response of the opposite sign was also found over the northern NAO node near Iceland but was not statistically significant. In a follow-on study, Gray *et al.* (2016) examined a much longer regional mslp dataset

extending back to 1660 and found a similar 3-4-year lagged response over the Azores region (see e.g., fig. 4 of Gray *et al.*, 2016). They also studied the intraseasonal evolution of the response and highlighted an NAO-like response at lag 0 in late winter (February) which they suggested was consistent with a top-down influence from the stratosphere via modulation of the polar vortex (e.g., Kodera & Kuroda, 2002) and an early-winter response (December) in the region of the Azores at lags of 3–4 years, consistent with a bottom-up response via modulation of NA SSTs (Scaife *et al.*, 2013). The same intraseasonal lagged evolution was also noted by Kuroda *et al.* (2022) who analysed the NAO index and found a positive NAO signal in February at the peak of solar forcing ($S_{\max}$) that appeared earlier in winter with increasing years following $S_{\max}$. However, there were also notable differences in their results. In particular, the peak SC response in their analysis, which employed the historical (1823–2016) NAO index rather than the mslp dataset, occurred at 1–2 year lags in contrast to the 3–4 years found in the mslp data (Gray *et al.*, 2013; Gray *et al.*, 2016).

Another reason that hampers a robust attribution is the short length of global atmospheric observational records in relation to the 11-year solar period, which means that relatively few cycles have been observed. In addition, the amplitude of the SC varies, and the surface response could be masked by natural variability during decades of weak solar activity, as in the early 20th century (e.g., see Chiodo *et al.*, 2019; Ma *et al.*, 2018). Improved confidence in detection and attribution can often be achieved using climate models that include one or more of the proposed mechanisms of solar influence (e.g., Drews *et al.*, 2022; Huo *et al.*, 2024; Spiegl *et al.*, 2023). However, while there has been some success in reproducing a lagged modulation of NA SSTs and mslp by the SC (Andrews *et al.*, 2015) most model SC responses in mslp are generally of weak amplitude and fail to reproduce the observed 3–4 year lag.

A growing number of recent studies have questioned the detection of an NAO response to 11-year SC forcing. For example, Chiodo *et al.* (2019) explored this using 20th Century Reanalysis datasets (1901–1997) and a climate model simulation. They noted the absence of a solar signal in the observed NAO prior to the 1960s and suggested that the apparent SC signal since the 1960s could occur by chance, based on their model simulation. However, we note that they chose to concentrate only on the two-year lagged response in their observational analysis because their focus was on the response in the NAO index. In addition, their model was unable to reproduce the observed SC response in the strength of the stratospheric polar vortex (see their supplementary material) which means that the proposed top-down SC influence was absent in their model. Spiegl *et al.* (2023) also questioned the veracity of a SC impact on the NAO. They examined multi-ensemble simulations of the Max Planck Earth System model and found that anomalies in mslp were independent of the imposed UV SC forcing and reflected internal variability of the troposphere. They also conducted a lead–lag correlation between the SC forcing and the NAO and suggested that any synchronisation between them (Thieblemont *et al.*, 2015) was likely a statistical artefact possibly influenced by internal decadal variability of the ocean. Nevertheless, as with the study by Chiodo *et al.* (2019), their model did not fully reproduce a SC influence on the stratospheric polar as seen in reanalysis, likely explaining the weak top-down forcing. Huo *et al.* (2024) subsequently investigated several different models and found a number of model biases that could contribute to this absence.

Thus, while model studies are valuable and clearly show the existence of decadal-scale variability in the troposphere-ocean system that is unrelated to SC forcing (see also James & James, 1989) there remains the need for further investigation into why they are unable to simulate the SC impact on the stratospheric polar vortex that is an essential part of the top-down influence mechanism. We note a corresponding challenge in modelling the polar vortex response to the QBO, which, in common with the top-down SC mechanism, also relies on the accurate modelling of wave–mean flow interactions in the stratosphere. Recent multimodel assessments of the so-called Holton–Tan relationship (Holton & Tan, 1980) have highlighted the inability of current climate models to adequately capture the strength of the polar vortex response and also the connection to the NAO (Anstey *et al.*, 2022). Further understanding and improved modelling of the QBO high-latitude response is therefore likely to benefit model studies of SC influence. An improved understanding of the magnitude of internal variability in fully-coupled Earth system models compared with their responses to external forcing, as highlighted by the signal-to-noise paradox (Scaife & Smith, 2018), would also be helpful.

In this paper we return to focus on analysing the available observational data to address the question of whether there is an NAO response to 11-year SC forcing. We examine two historical mslp datasets from the 20CRv3 reanalysis and the ERA5 reanalysis (see Section 2). In their analysis of the HadSLP mslp dataset Gray *et al.* (2013, 2016) found a statistically significant DJF SC response over the southern (Azores) node of the NAO but not over the northern (Icelandic) node. The absence of a statistically significant response over Iceland could be due to larger background variability, as suggested by Gray *et al.* (2013), or it could be that the SC forcing does not invoke a response in the NAO, as suggested in more recent papers (Chiodo *et al.*, 2019; Spiegl *et al.*, 2023). To investigate this, we use

multiple linear regression (MLR) analysis as previously employed by many authors, but first we isolate the major modes of NA variability using an empirical orthogonal function (EOF) analysis so that the solar response in the NAO (EOF-1), the East Atlantic (EA) pattern (EOF-2) and the Scandinavian pattern (EOF-3) can be separated. Section 2 describes the datasets and methodologies used in the study. Section 3 presents the results of the study and compares them to previous work. Section 4 provides a summary and discussion of the results.

2 | DATA AND METHODOLOGY

2.1 | Datasets

This study employs two atmospheric reanalyses datasets to examine the SC signatures in mslp in the NA region. The NOAA-CIRES-DOE 20th Century Reanalysis version 3 (20CRv3) dataset provides global estimates of the atmosphere from 1806 to 2015 using only surface pressure observations and prescribing the HadISST2 SSTs, sea ice concentration and the CMIP5 radiative forcings (Slivinski *et al.*, 2019). This dataset was built as an ensemble (80 members derived from eight distinct SST initialisations) and is released as a best estimate of the mean together with an uncertainty measure (Fujiwara *et al.*, 2017). SC forcing is present in the model employed to produce the 20CRv3 dataset, with prescribed TSI variations, but the spectrally resolved solar irradiance (SSI) variability and associated solar variations in stratospheric ozone are neglected. As a result, SC signals in the 20CRv3 stratosphere are negligible (Misios & Schmidt, 2013). Note, however, that because mslp observations are assimilated into the model any diagnosed SC variability in the mslp field can be attributed to the assimilation and not to the model's SC forcing. For this reason, the 20CRv3 shows very similar mslp SC response results to actual mslp observations over the 1850–2015 period analysed in previous studies (e.g., HadSLP2r as in Gray *et al.*, 2013). Since (a) the density of marine mslp observations over the NA prior to the 20th century is very low (Allan & Ansell, 2006) and (b) SC amplitudes were weak in the late 19th century, we restrict our study of the 20CRv3 dataset to the period 1900–2014, as in Chiodo *et al.* (2019).

We additionally examine the SC signal in the ECMWF ERA5 reanalysis (Hersbach *et al.*, 2020) which covers the recent period. The ERA5 dataset is produced by assimilating not only surface data but also an extensive array of upper-air meteorological observations. It therefore represents our best current estimate of the state of the atmosphere with an improved representation of the stratospheric circulation, particularly after 1979 when satellite observations were introduced into the assimilation procedure. We examine the SC signals in the ERA5 dataset over the period 1941–2022. We note that ERA5 and 20CRv3 give very similar results over the common 1941–2014 period, providing confidence that differences between reanalyses reported later are attributed to the different periods considered and not to the different datasets.

2.2 | Methodology

The approach taken in this paper is first to isolate well-known modes of variability in the NA region by applying an EOF analysis and then to regress out possible SC signatures with a MLR model. In this way, the EOF analysis pre-filters the boreal winter mslp time series and in addition it provides a linear decomposition of the solar response to the leading modes of variability in the NA region. This methodology differentiates from previous studies which used MLR on unfiltered mslp data to extract the SC contribution, and we argue that the spatiotemporal EOF filtering provides an insight on the interplay of different leading modes in the years following $S_{\max}$.

We first perform the EOF analysis to identify the five leading patterns of December–January–February average (DJF) mslp variations in the NA region, defined between 20°–80° N and 90° W–40° E (Hurrell *et al.*, 2003). Prior to the EOF analysis, we weight the SLP anomalies by the square root cosine of latitude to ensure that data points near the pole do not have a disproportionate impact on the analysis. EOF analysis separates the variability of the mslp into orthogonal modes, with the first mode containing the largest proportion of the variability, and each subsequent mode containing progressively less. The first three leading EOF modes of mslp for 20CRv3 are shown in Figure 1 and describe well-known patterns of the wintertime variability (Cassou *et al.*, 2004). The spatial pattern of the first EOF explains 44% and shows the well-understood north/south dipole of negative/positive anomalies associated with the NAO. The second leading mode (EOF-2) of mslp explains 19% and shows the spatial distribution of the East Atlantic (EA) pattern, which features a northward extension of the Azores high (Wallace & Gutzler, 1981). The third leading mode (explains 12%) resembles the Scandinavian (SCAND) pattern and appears in the selected domain as a see-saw with a primary anticyclonic anomaly over the Scandinavian Peninsula and a cyclonic anomaly over the northeastern Atlantic.

Once the EOF has been performed, we reconstruct the mslp time series by retaining only the first five EOFs and the associated principal components (referred to as

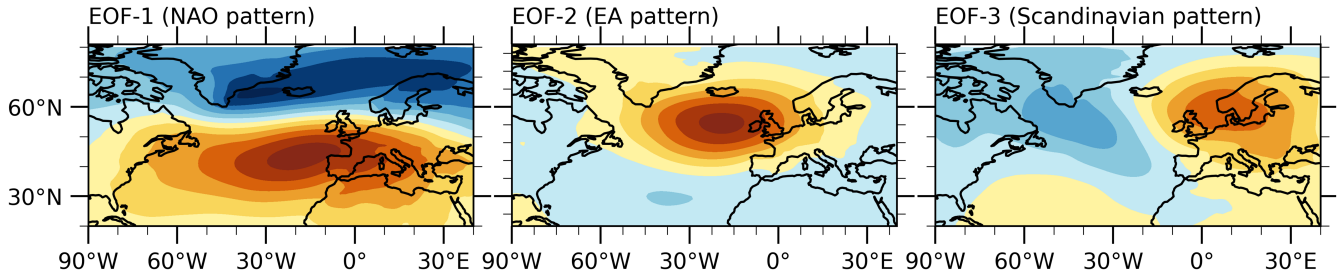

FIGURE 1 The first three leading empirical orthogonal function (EOF) patterns of the December–January–February average (DJF) mslp from 20CRv3 for the 1900–2014 period. EOFs 1,2,3 capture the North Atlantic Oscillation (NAO), the East Atlantic (EA) and the Scandinavian patterns (SCAND), respectively. [Colour figure can be viewed at wileyonlinelibrary.com]

EOF-reconstructed dataset hereafter). The first five EOFs account for almost 84% of the total variance. Additionally, we reconstruct the mslp for EOF-1, EOF-2 and EOF-3, separately, to analyse the time series associated with the NAO, EA and SCAND patterns, respectively. This allows us to perform a detailed investigation of the solar signals in the NA using MLR analysis to separate the SC in the individual leading modes and how they superimpose to give the pattern of 3–4 year. lagged response seen previously in the wintertime mslp (Gray *et al.*, 2013). In addition, the relative contribution of the NAO and EA response in the early/late-winter SC response is explored by analysing November–December (ND), December–January (DJ), January–February (JF) and February–March (FM) averages. For every two-month average, a separate EOF analysis is performed.

The lead/lag MLR analysis employed in the study has been widely used in the literature (Frame & Gray, 2010; Gray *et al.*, 2013; Kuroda *et al.*, 2022; Lean & Rind, 2008; Ma *et al.*, 2018; Misios *et al.*, 2016). We built the MLR model based on the Generalised Least Square estimation to properly treat heteroskedasticity and auto-correlation (GLSAR in python package *statsmodel*). The MLR assumes an auto-regressive term in the residuals and transforms possibly correlated errors through an interactive process to new terms that are serially uncorrelated and homoscedastic. A similar MLR model has been applied in Kuchar *et al.* (2017) to isolate SC signals from other forcings in the lower tropical stratosphere, and here it is amended to include time lags for the SC predictor. All MLR regression coefficients are scaled to $1\,W{\cdot}m^{-2}$ increase in TSI, which is a typical increase from solar minimum to maximum. The statistical significance of the resulting regression coefficients against the null hypothesis of zero regression coefficient is rejected with $p < 0.05$ (0.1) using a two-tailed *t*-test, which corresponds to the 95% (90%) confidence level. Because the EOF reconstruction is based on the same principal component time series, the significance testing in single-mode EOF reconstructions (e.g., NAO, EA and SCAND) returns the same *p*-values at all grid points. This means that SC signals in single-mode reconstructions are significant (or not) at all grid points.

The MLR model uses multiple forcing indices (predictors) to describe solar variations as well as additional sources of climate variability in the NA region. The 11-year SC is characterised by a detrended TSI predictor using a band-pass Butterworth filter to retain periodicities smaller that 18 years, as described in Misios *et al.* (2016). Kuroda *et al.* (2022) applied a similar filtering of the multidecadal TSI variations. Other analyses (e.g., Gray *et al.*, 2013) have used observations of the solar sunspot number instead, but we note that the resulting SC signals are not sensitive to the choice of the solar predictor because of the high correlation of the annual detrended TSI and sunspot numbers. This is not the case for the unfiltered-TSI, which embeds a long-term positive trend over the 20th century not apparent in the sunspot record. In addition to the 11-year SC, a set of predictors that capture well-known sources of climate variability in the NA region is also included in the MLR. The choice of these predictors follows previous MLR studies (Frame & Gray, 2010; Gray *et al.*, 2013; e.g., Misios *et al.*, 2016; Ma *et al.*, 2018) and they are briefly listed here: (a) a globally averaged stratospheric aerosol optical depth at 550 nm (Sato *et al.*, 1993) to represent major volcanic eruptions, (b) CO_2 equivalent concentrations of all greenhouse gases, and (c) a band-passed filtered (4–8 years) SST-based Nino3.4 index to represent the El Nino–Southern Oscillation variability. The quasi-biennial oscillation (QBO) is known to have significant surface impacts (e.g., García-Franco *et al.*, 2022) but observations of the QBO do not extend sufficiently far back in time to provide an index to analyse the longer historical periods from 1900. In this case, the QBO forcing index was excluded, following the approach of Gray *et al.* (2016). We also considered an SST-based index of the Atlantic Multidecadal Variability but we found negligible sensitivity of the MLR results and it was finally excluded in the MLR model.

In Figure 6 below we show the time evolution of the mslp amplitude of the main SC anomaly found over

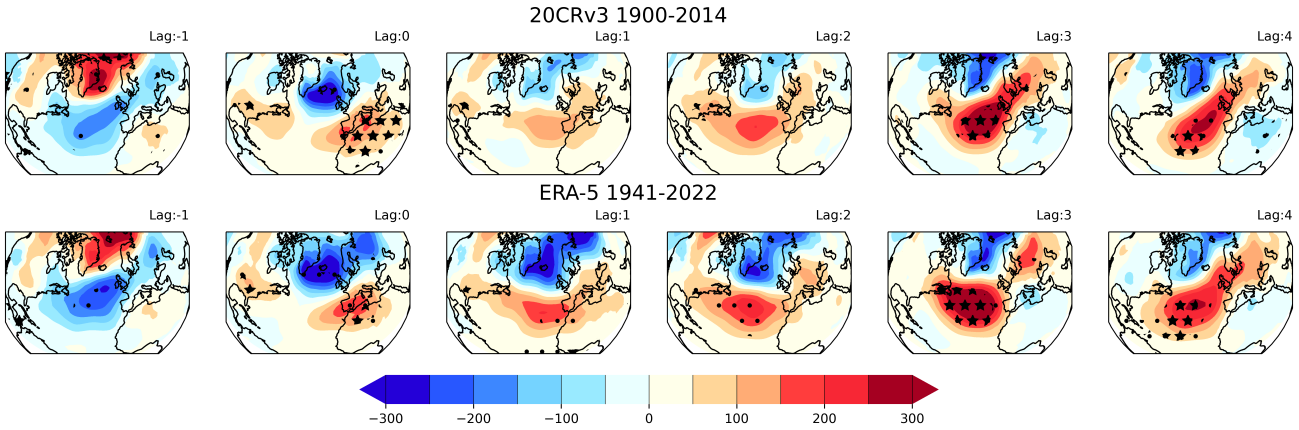

FIGURE 2 Eleven-year solar-cycle response from multiple linear regression (MLR) analysis of December–January–February average (DJF)-mean mean-sea-level pressure (mslp) (units: Pa·1 W^{-1}·m^{-2} total solar irradiance [TSI] increase) in reanalyses. Top row: 20CRv3 for 1900–2014, bottom row: ERA5 for 1941–2022. The columns show results at different lags from −1 to +4 years following S_{max}. Statistical significance is indicated by black stars (dots) for $p < 0.05$ (0.1), respectively, using a two-tailed t-test. [Colour figure can be viewed at wileyonlinelibrary.com]

the Azores region in the DJF analysis. The figure shows the monthly-averaged amplitude at 50° N and 25° W, which corresponds to the core of the positive response seen in Figure 2 at lag +3 years. Sensitivity tests (not shown) were performed to check that the results were not sensitive to small variations in the selected location.

3 | RESULTS

3.1 | Solar cycle signatures in winter mean-sea-level pressure

To compare the surface impacts of the SC on NA climate with results from previous studies, Figure 2 presents the lagged solar regression responses for the unfiltered mslp from the 20CRv3 and ERA5 reanalysis datasets. Note that the datasets cover different, partially overlapping, periods. As already noted (see Introduction), an NAO-like response pattern is seen to evolve following S_{max}, consisting of a dipolar structure with a positive response of approximately 3 hPa over the Azores region that peaks at lags of 3–4 years and a slightly weaker, statistically insignificant negative response over the polar regions. The response in 20CRv3 (top row) and the ERA5 analysis (bottom row) both show a consistent response with statistical significance at lag +3 and lag +4 years despite the fewer SCs under consideration in the latter dataset.

While the primary positive mslp response resembles the positive node of the NAO pattern, we note that the maximum positive response is not centred directly over the Azores but is positioned slightly to the north and the positive anomaly at lags of +3–4 years extends northward and eastward towards Scandinavia. This is also seen in the results of Gray *et al.* (2016) (see their Fig. 3 at lag +3 years). The maximum signal being slightly to the north of the Azore plus the fact that there is no statistically significant response over the northern node of the NAO, suggests that the solar signal does not project directly onto the NAO pattern of variability. The anomaly pattern associated with the EA mode of variability shares a similar maximum anomaly positioned to the north of the Azores (see e.g., Figure 1 above, and fig. 3 of Hall & Hanna, 2018). This suggests that the solar response could be a more complex superposition of responses onto several leading modes of winter variability, a possibility that is explored in the following sections.

3.2 | Solar-cycle signatures in the empirical orthogonal function-reconstructed mean-sea-level pressure

Figure 3 presents the lagged solar regression responses for the EOF-filtered mslp data, reconstructed by considering the first five EOFs. The mslp solar responses compare well with Figure 2 and the corresponding figure in Gray *et al.* (2013), and in both the 20CRv3 and ERA5 a significant mslp response exceeding 95% (90%) confidence level is identified at lag +3 (lag +2) years, with magnitudes exceeding 3 hPa. This means that SC signatures project mostly on the leading atmospheric models. The shorter ERA5 period generally indicates stronger anomalies. This could be related to a better representation of mslp variability, stronger SC forcing and possibly an influence of warmer background temperatures in the latter half of the century. We also note the absence of the high significance over North Africa detected in the 20CRv3 at lag 0 years

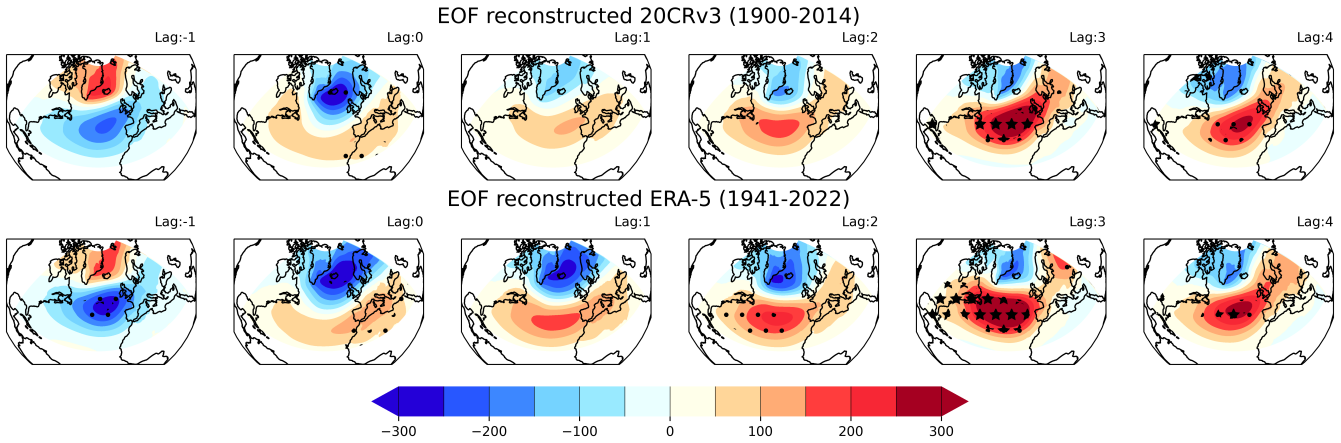

FIGURE 3 Eleven-year solar-cycle response for December–January–February average (DJF) mean-sea-level pressure (mslp) from multiple linear regression (MLR) analysis of empirical orthogonal function (EOF)-reconstructed time series (units: Pa·1 W^{-1}·m^{-2} total solar irradiance [TSI] increase). The EOF reconstruction is based on the first five leading modes. Top row: 20CRv3 for 1900–2014; bottom row: ERA5 for 1941–2022. The columns show results at different lags from −1 to +4 years following S_{max}. Statistical significance is indicated by black stars (dots) where $p < 0.05$ (0.1) respectively, using a two-tailed t-test. [Colour figure can be viewed at wileyonlinelibrary.com]

in Figure 2, implying the contribution of higher modes of variability.

The spatial pattern of the detected SC signature at lag 0 years shows little similarity to the NAO pattern, as the signal peaks over the Mediterranean. Only at lag +1 year is a strong dipole of mslp anomalies established over the typical NAO centres of action, while at lags of +3, 4 years the positive anomalies are displaced northward and extend towards Scandinavia. In the ERA5 analysis at lag +3 years in particular, the position of the maximum anomaly in the reconstructed pattern is very similar to the EA pattern distribution. This is also seen in Figure 2, but the EOF filtering provides better evidence for a superposition between, at least, the EOF-1 and EOF-2 patterns (NAO and EA, respectively), in shaping the SC signature over the different lags. This superposition is investigated in the following sections by performing the MLR analysis on the individual leading modes, that is, the NAO, EA and SCAND dipoles corresponding to the three leading EOFs (see Section 2.2). We note that the variance associated with EOF-2 and EOF-3 is comparable and in the analysis of individual two-month averages (next section) they sometimes switch so that the Scandinavian dipole has greater variance than the EA pattern. For this reason, we choose to refer to the solar responses in the named variability patterns, rather than referring to EOF-2 or EOF-3, to avoid confusion.

3.3 | Solar cycle signatures in leading patterns of North Atlantic variability

In Figure 4 the 11-year DJF SC responses in the three leading patterns of variability are shown for the 20CRv3 dataset for the period 1900–2014. There is no statistically significant 11-year SC response in the DJF NAO pattern (top row). There is, however, a statistically significant response, exceeding 90%, in the EA pattern (middle row), with a (non-significant) negative EA anomaly at lag 0 and lag −1 year and a corresponding (statistically significant) positive response that peaks at lag +3 years. No statistically significant response is evident in the Scandinavian dipole (bottom row) or in the higher EOFs (not shown). By superposing the responses in NAO and EA patterns it is easy to understand the origins of the overall statistically significant response at lags of +3–4 years, since they have the same sign in the region of the Azores and to the west of the United Kingdom and hence reinforce each other at lags of +3–4 years but have opposite signs at lag 0 years.

Figure 5 shows the corresponding SC response in the NAO/EA/SCAND patterns of variability from the ERA5 dataset over the period 1941–2022. The patterns of response in both the NAO and EA are similar to those of the 20CRv3 dataset but the NAO response is stronger than in the 20CRv3 dataset and peaks earlier at lags 0 and +1 years. Despite the stronger magnitude the NAO signal remains below 90% significance over the ERA5 period. The EA response shows a time dependence similar to the 20CRv3 but is weaker and no longer statistically significant at lag +3 years.

The evolving pattern, which is captured in both reanalyses, suggests an initial NAO-like response that commences at lag 0 years together with a substantial contribution from the EA pattern that lags by a quarter cycle and hence boosts the overall signal at lag +3 years. Similar patterns of response are also seen in the corresponding analysis using the HadSLP dataset for the

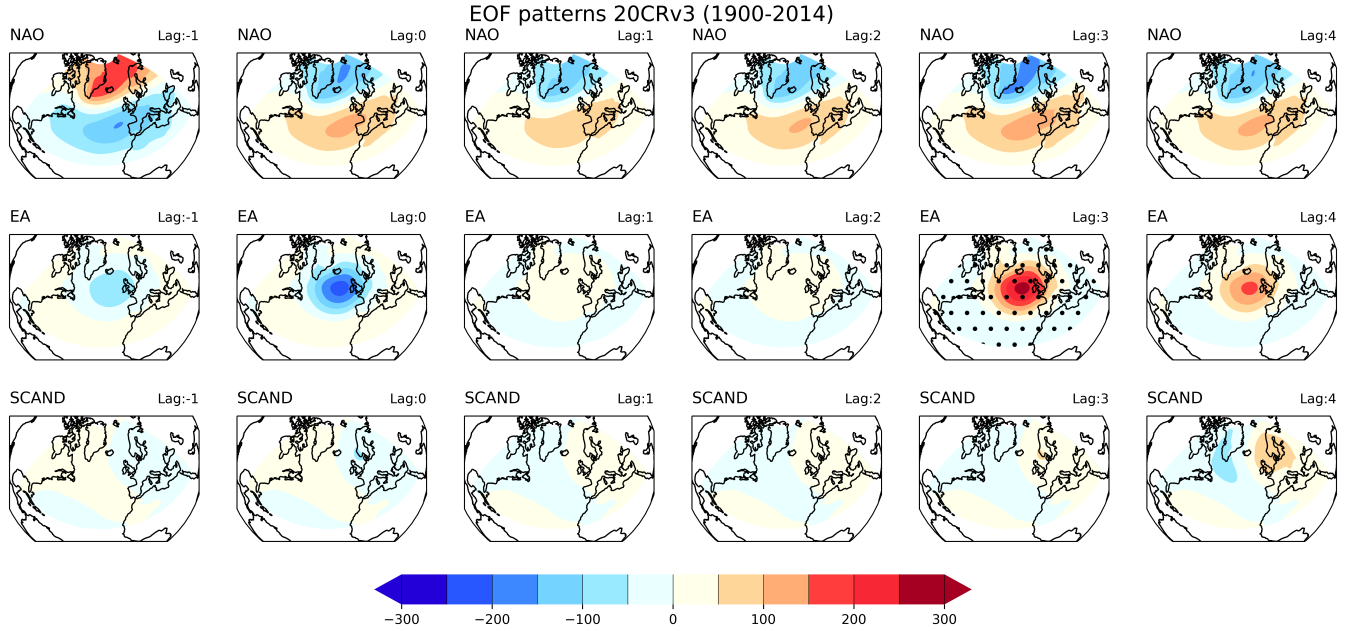

FIGURE 4 Eleven-year solar-cycle response for December–January–February average (DJF) mean-sea-level pressure (mslp) from multiple linear regression (MLR) analysis of individual empirical orthogonal function (EOF)-reconstructed time series (units: Pa·1 W^{-1}·m^{-2} total solar irradiance [TSI] increase) using the 20CRv3 dataset for the period 1900–2014. Top/middle/bottom rows show the responses associated with the NAO (EOF-1), EA (EOF-2) and Scandinavian dipole (EOF-3) patterns of variability, respectively, while the columns show the different lags from −1 to +4 years following S_{max}. Statistical significance is calculated by considering the corresponding principal components and is the same for the whole domain. Statistical significance is indicated by black stars (dots) denoting $p < 0.05$ (0.1) respectively, using a two-tailed t-test. [Colour figure can be viewed at wileyonlinelibrary.com]

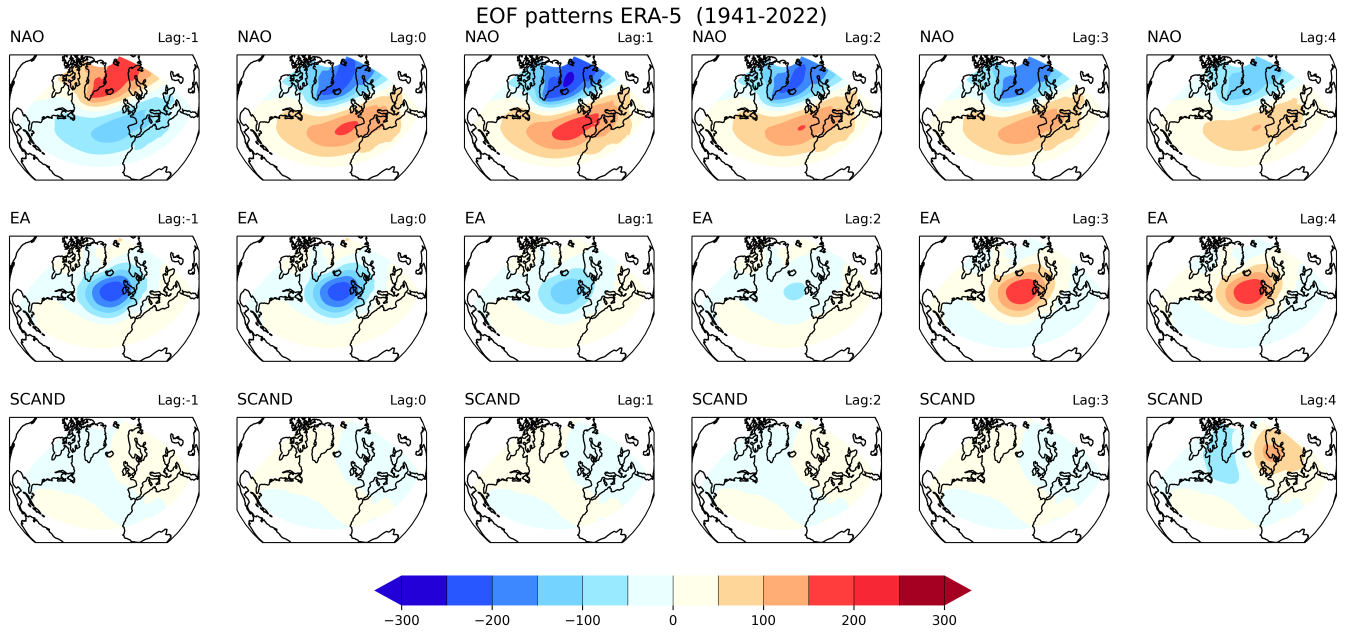

FIGURE 5 As Figure 4 but using ERA5 over the period 1941–2022. [Colour figure can be viewed at wileyonlinelibrary.com]

period 1900–2014 (not shown) but the responses are not statistically significant at the 95% confidence level.

The decomposition of the SC signature into the individual leading EOF patterns helps to understand the mslp responses seen in Figures 2 and 3. This is also demonstrated in Figure 6, which shows the evolution of the amplitude of the mslp SC anomaly at 50° N and 25° W, corresponding to the core of the positive response seen in

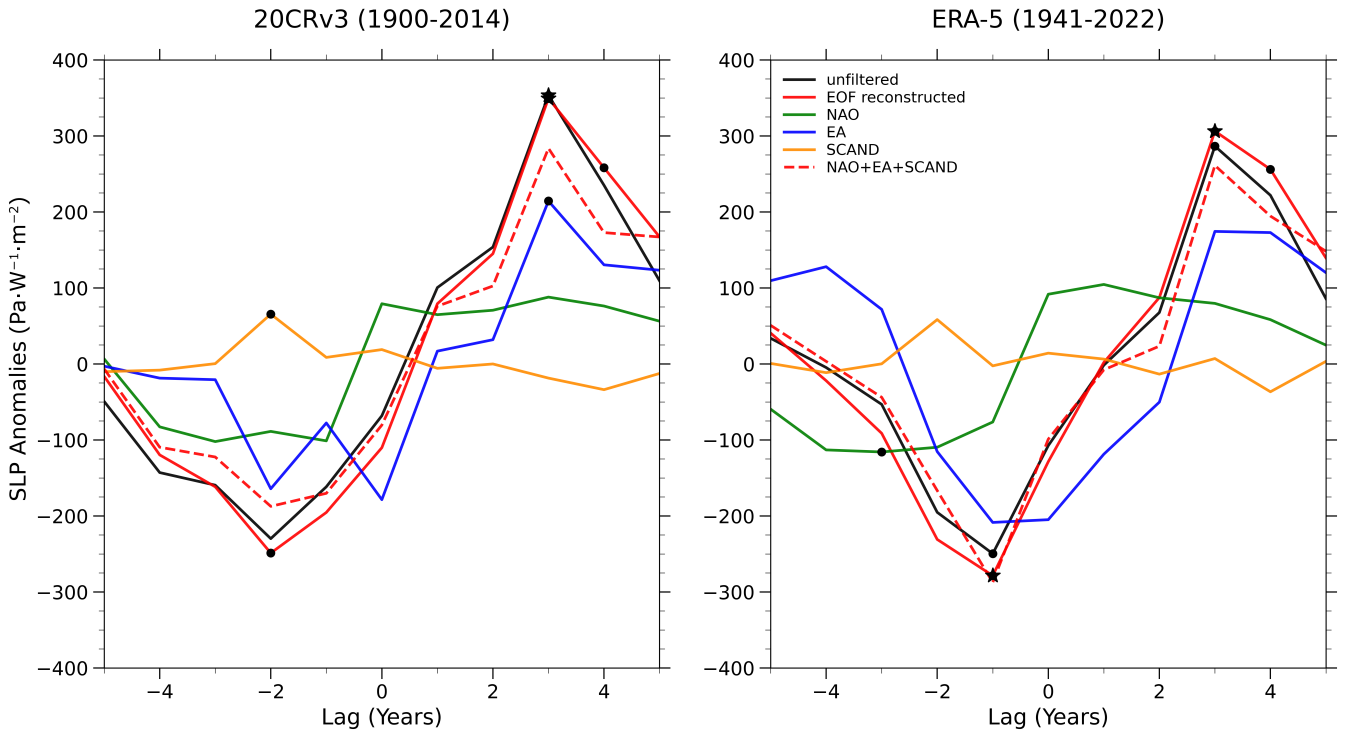

FIGURE 6 Eleven-year solar-cycle response in December–January–February average (DJF) mean-sea-level pressure (mslp) (Pa·1 W^{-1}·m^{-2}) from multiple linear regression (MLR)analysis at 50° N and 25° W for the unfiltered mslp (black), the reconstructed mslp that retains the five leading EOFs (red), the individual responses in the North Atlantic Ocean (NAO) (green), East Atlantic (EA) (blue) and Scandinavian (SCAND) (orange) patterns and the sum of these three leading EOFs (dashed red). The X-axis shows the lag from −5 to +5 years following S_{max}. Left: 20CRv3 for 1900–2014; right: ERA5 for 1941–2022. Statistical significance is indicated by black stars (dots) denoting $p < 0.05$ (0.1), respectively, using a two-tailed t-test. [Colour figure can be viewed at wileyonlinelibrary.com]

Figure 2 at lag +3 years. As discussed earlier, a significant increase of mslp at lag +3 years (>3 hPa) is also captured in the mslp reconstruction that retains the first five leading modes (compare the unfiltered and EOF-reconstructed responses in Figure 6). The figure demonstrates that the NAO (solid orange line) lags the peak in solar forcing by about 1 year but the lagged mslp response documented in earlier studies which peaks at lag +3 years in both the 20CRv3 and ERA5 datasets is primarily associated with the EA pattern (solid pink line). The NAO explains about 25% of the total unfiltered response, whereas the EA explains 60%. The sum of the first 3 EOFs (dashed red line) explains almost 80% of the total unfiltered response in 20CRv3. This is also evident in the 1941–2022 period, where the MLR analysis identifies a pronounced increase in the EA contribution that surpasses the NAO amplitude at lags of +2–5 years. The NAO explains merely 25% whereas the EA explains 60% of the total unfiltered response in ERA5. The Scandinavian pattern shows only a weak contribution to the overall mslp DJF response in the NA region.

It is not immediately obvious why the ERA5 analysis shows a stronger NAO response at lag 0 years and a weaker EA response at lag +3 years than the 20CRv3 analysis. It could be due to the different input data used in preparation of the datasets or it could be due to the different timespans of the datasets. To test this, the 20CRv3 analysis was repeated using only the period 1941–2014, to match the time period as closely as possible to the ERA5 period (not shown). The results were very similar to those from the ERA5 analysis, confirming that the different time period is primarily responsible for the difference in dominance of the NAO and EA patterns.

In summary, the EOF analysis of the DJF mslp shows no statistically significant 11-year SC response in the NAO. However, a previously unrecognised 11-year SC response in the EA pattern was found with a positive mslp anomaly at lags of +3–4 years which reinforces the NAO response, resulting in an overall response that is statistically significant at those lags, in agreement with previous studies. The EA response appears to be stronger in the early part of the period examined (pre-1941), but its statistical significance is not high. Previous studies have suggested that there may be different processes acting in early/late winter so that analysing the combined DJF months may hide conflicting responses. A weaker subpolar gyre or altered external forcing regimes in the pre-1941 period may have enhanced EA mode variability, potentially amplifying the solar signal

response (e.g., Huo *et al.*, 2024). For this reason, we now examine the early and late winter responses separately.

3.4 | Early/late winter solar-cycle signatures

The studies of Gray *et al.* (2016) and Ma *et al.* (2018) noted that the early winter 11-year SC response in mslp was different to the late winter response (see also Kuroda *et al.*, 2022). The early-winter response was found to maximise at lags of +3 years while the later winter response maximised at lag 0 years. Gray *et al.* (2016) proposed that this was consistent with a top-down mechanism via the strength of the stratospheric vortex at lag 0 years together with an amplifying re-emergence mechanism via Atlantic SSTs (Scaife *et al.*, 2013) that perpetuates the SC response and peaks at lags of a quarter-cycle, that is, approximately +3 years. They proposed that since the Northern Hemisphere stratospheric vortex tends to show greatest variability in late winter and its impact at the surface can last for several months (Baldwin & Dunkerton, 2001) it is most likely to impact the late winter months while the re-emergence mechanism that carries the SC anomaly from one winter through to the next is more likely to be evident in early winter months. Kuroda *et al.* (2022) who studied the historical station-based NAO index (Jones *et al.*, 1997) also found similar intraseasonal variations, with a maximum positive NAO signal in late winter (February) at the peak of solar forcing (i.e., at lag 0) that appeared earlier in winter with increasing years following S_{max}. However, the latter response peaked at lags of +1–2 years rather than +3–4 years, possibly because of differences in derivation of their NAO index or the different timespan examined (see Introduction).

To explore the early/late winter responses in the individual EOF patterns, we first examine the ERA5 MLR analysis results (1941–2022). Figure 7 shows the 11-year SC response in the NAO for November–December (ND), December–January (DJ), January–February (JF) and February–March (FM) averages, respectively. It is evident that the (statistically insignificant) NAO response in the

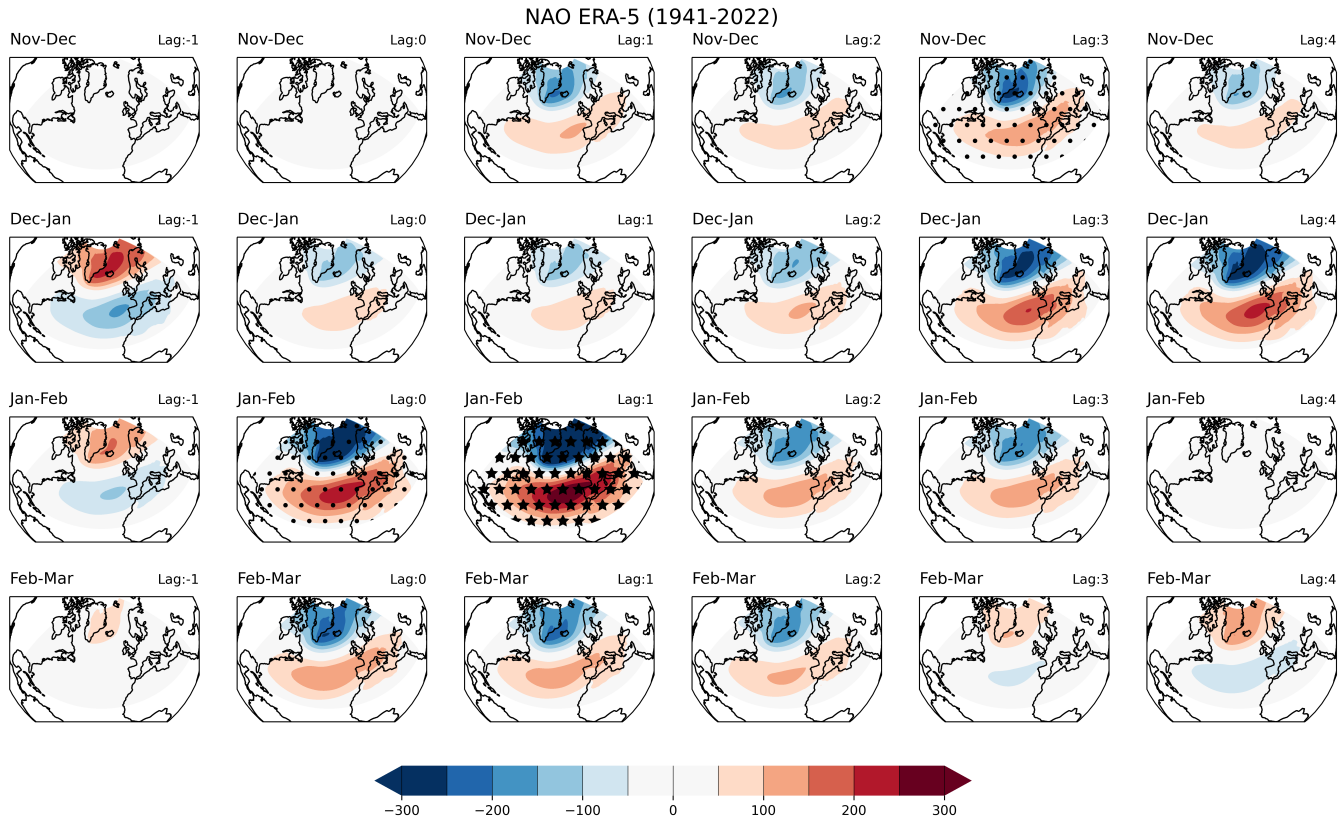

FIGURE 7 Eleven-year solar-cycle response from multiple linear regression (MLR) in the North Atlantic Oscillation (NAO) reconstructed mean-sea-level pressure (mslp) using the ERA5 dataset for the period 1941–2022. Top to bottom rows for November–December, December–January, January–-February and February_March averages. The columns show the different lags from −1 to +4 years. following S_{max}. Statistical significance is calculated by considering the corresponding principal components and pertain to the whole domain. Units are Pa·1 W^{-1}·m^{-2} total solar irradiance [TSI] increase. Statistical significance is indicated by black stars (dots) denoting $p < 0.05$ (0.1), respectively, using a two-tailed *t*-test. [Colour figure can be viewed at wileyonlinelibrary.com]

DJF analysis of Figure 5 at lag 0 and +1 years originates primarily from the late winter (JF) months. Unlike the DJF response, the NAO response in JF at lag +1 year is statistically significant at the 95% confidence level. Its amplitude exceeds 3 hPa, which is a substantial proportion of the total variance in mslp at this time of the year (see e.g., Gray *et al.*, 2013). This agrees reasonably well with Kuroda *et al.* (2022) who found the peak NAO response in February at lag 0. The corresponding analysis of the SC signal in the NAO from the 20CRv3 dataset is shown in Figure 8. It shows a similar late-winter solar response at lags of 0 and +1 years although, as already seen in the DJF results, the addition of the earlier years (pre-1941) has weakened both the amplitude and the statistical significance.

In addition to the late-winter SC response at lag 0 and +1 years there is also a statistically significant SC response in the NAO in early winter at lags +3–4 years. This is particularly evident in the 20CRv3 analysis where it is statistically significant at the 95% (90%) confidence level in ND at lag +3 years over both the Icelandic and Azores regions in the 20CRv3 (ERA5) analysis respectively. The amplitude of this response exceeds 1.5 hPa which is smaller than the lag 0 response in late winter but nevertheless still a substantial proportion of the total variance. This is again consistent with the results of Kuroda *et al.* (2022) who also found that the maximum response occurred earlier in the winter as the lag was increased, although their peak statistically significant response occurred at +1–2 years rather than the +3–4 years found here.

In summary, by examining the early and late winter responses separately, instead of using the traditional DJF-average, statistically significant SC responses in the NAO are clearly revealed.

The 11-year solar responses in the EA mslp pattern for the ERA5 and 20CRv3 analyses are shown in Figures 9 and 10, respectively. The EA patterns show a very different evolution to the NAO pattern. A statistically significant response is only seen in the late winter, with a positive anomaly peaking at lags of +3 and +4 years (only statistically significant in the ERA5 dataset) and a corresponding negative anomaly centred half a cycle later (around lag +9 years, not shown) which is still clearly evident at lags of −1 years and lag 0 years. The DJF solar response in the EA pattern shown in Figure 4 can thus be seen to originate primarily from the late winter, although the statistical significance of these results is clearly limited and there are also differences in details of the response between the two datasets. These differences are most evident in the February–March responses, with the ERA5 showing a strong, statistically significant response at lags of −1 years and +3 years while the 20CRv3 shows a very weak

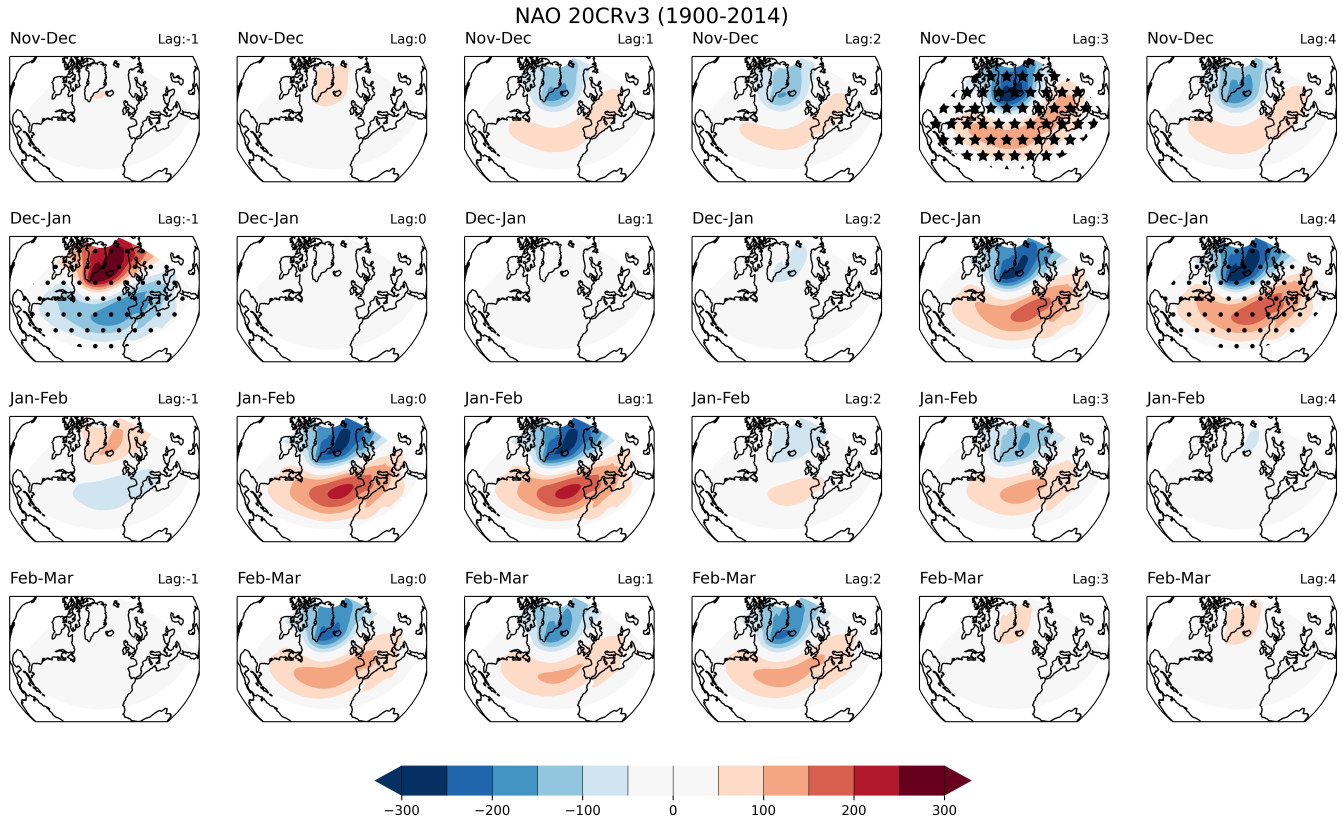

FIGURE 8 As Figure 7 but for 20CRv3 dataset (1900–2014). [Colour figure can be viewed at wileyonlinelibrary.com]

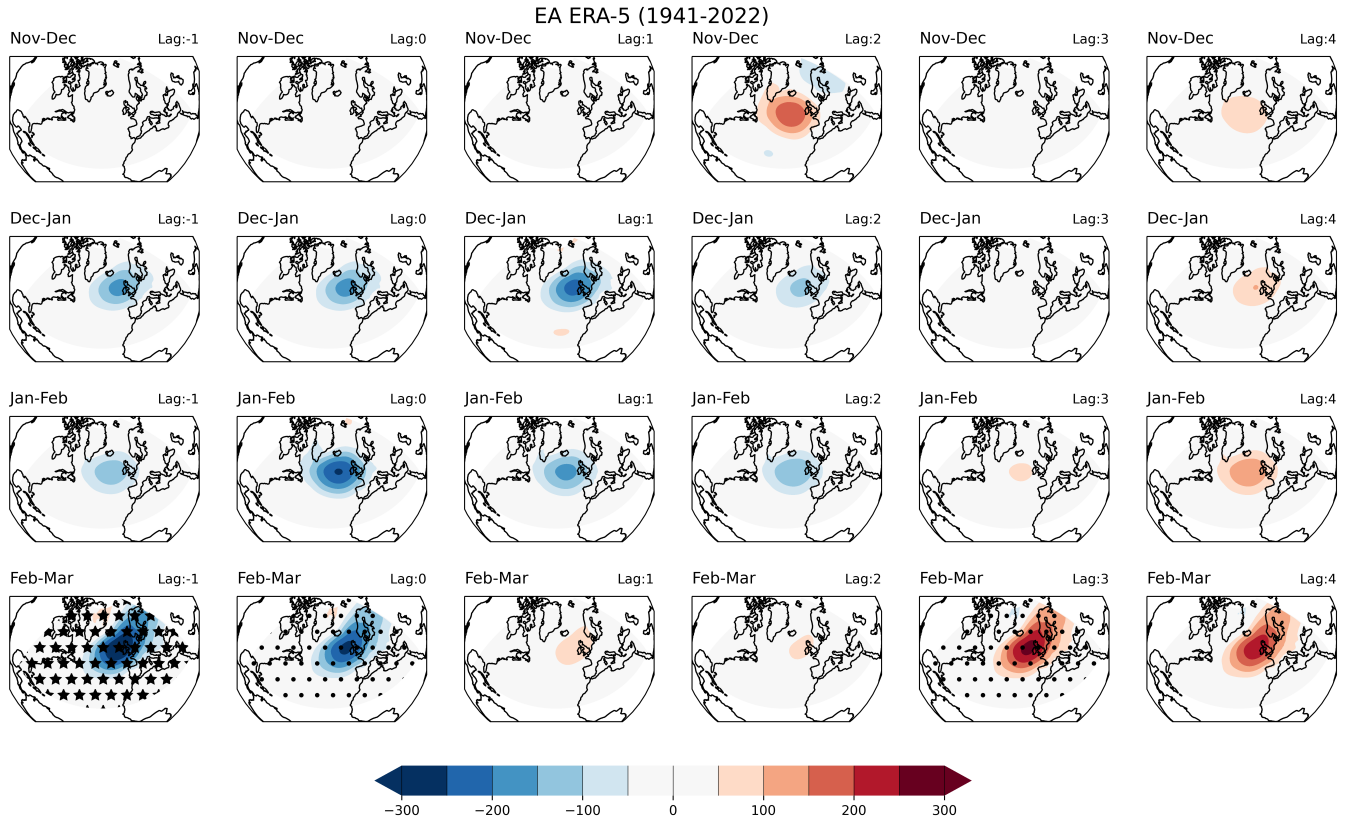

FIGURE 9 As Figure 7 but for the East Atlantic (EA) pattern. [Colour figure can be viewed at wileyonlinelibrary.com]

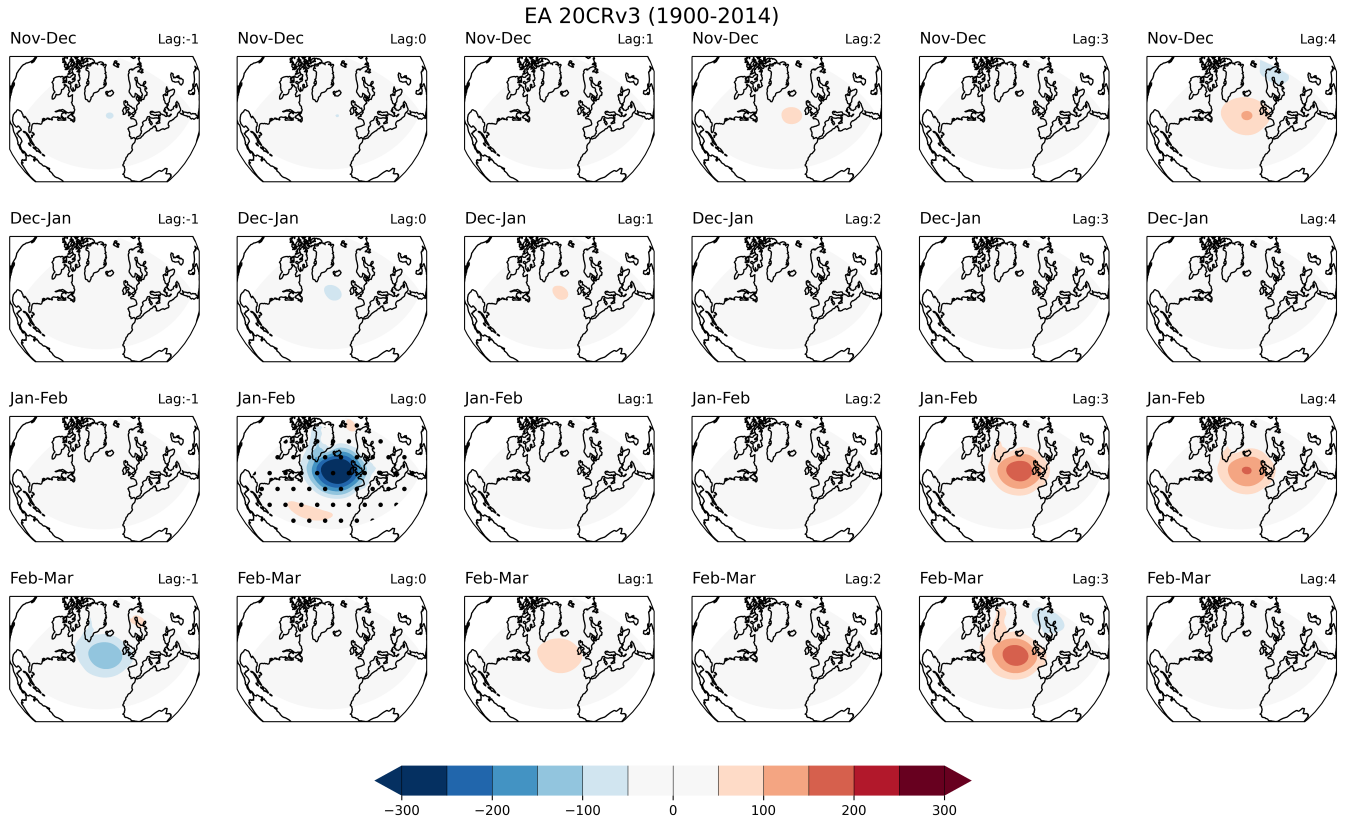

FIGURE 10 As Figure 8 for East Atlantic (EA) but for 20CRv3 dataset (1900–2014). [Colour figure can be viewed at wileyonlinelibrary.com]

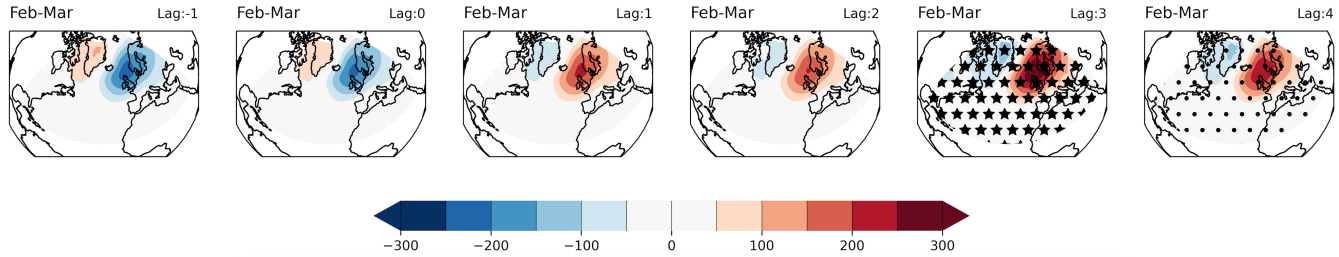

FIGURE 11 Eleven-year solar-cycle response from multiple linear regression (MLR) in the Scandinavian (SCAND) reconstructed mean-sea-level pressure (msl)p using the 20CRv3 dataset for the period 1900–2014. Ony February–March averages are shown. The columns show the different lags from −1 to +4 years. following S_{max}. Units are Pa·1 W^{-1}·m^{-2} total solar irradiance [TSI] increase. Statistical significance is indicated by black stars (dots) denoting $p < 0.05$ (0.1), respectively, using a two-tailed t-test. [Colour figure can be viewed at wileyonlinelibrary.com]

response. We note that the EOFs have been calculated for each two-month average and the FM average EOF2 pattern in ERA5 (not shown) is slightly different from the traditional EA pattern identified in the other two-month and DJF averages. It extends northeasterly from the west of Ireland towards Scandinavia and thus resembles a combination of the EA and Scandinavian patterns, likely explained by a mixing of the leading modes. This is clearly apparent in Figure 9. This mixing is less evident in the 20CRv3 dataset, where Figure 10 shows a more traditional EA pattern with a single maximum to the west of Ireland. Figure 11 shows the 11-year solar response in the Scandinavian pattern from the 20CRv3 analysis in the months February–March (there is no SC response in this mode in any other of the winter months). It shows a strong, statistically significant response at lags of +3 years that stretches from the west of Ireland to Scandinavia, similar to the EA response at the same lag in the ERA5 dataset. The 11-year solar response in the EA/Scandinavian patterns of the two datasets is therefore not so dissimilar as it appears at first sight. This response in the EA/Scandinavian pattern also helps to understand the origin of the DJF responses shown in Figure 2, in which there is an elongation of the response towards Scandinavia at lags of +3 and +4 years.

4 | SUMMARY AND DISCUSSION

This study has examined a set of reanalyses, both modern ECMWF-ERA5 and NOAA-CIRES-DOE 20th Century (20CRv3), to evaluate the robustness of the signatures of the 11-year SC in the surface wintertime NA climate. The approach has been different to previous studies by first performing an EOF analysis to allow examination of the separate responses in the NAO, the EA and the Scandinavian patterns of variability before performing the usual multilinear regression analysis to isolate the SC signal. Consistent with earlier studies (e.g., Gray *et al.*, 2013), the DJF SC response in 20CRv3 and ERA5 is mainly characterised by positive anomalies in mslp in the region slightly to the north of the Azores at lags of approximately +3 years that contribute to a positive NAO-like pattern. A statistically significant SC response was not found in the combined DJF NAO, but when the response was examined separately for the early/late winter months a statistically significant NAO response was found at both lag 0 years in late winter (JF/FM) and at lag +3 years in early winter (ND/DJ). These results are consistent with those of Gray *et al.* (2016) and Kuroda *et al.* (2022), although the latter found the peak response in early winter at slightly smaller lags (+1–2 years), which is likely explained by the different periods analysed. Our results also suggest that an NAO-like response should not be anticipated throughout all winter months but is predominately a late-winter response at lag 0 years. The study also reconciles with the findings of Chiodo *et al.* (2019) for an insignificant SC response in the NA climate, since we have also found low statistical significance of the mean DJF mslp anomalies to SC forcing over the 20th century.

Nevertheless, we find that the NAO response is not the key ingredient of the mslp SC response at lag +3 years. Instead, we find that the EA pattern (EOF-2) is the primary contributor, with a substantial, statistically significant contribution in late winter (JF/FM). We find that the lag +3 years DJF SC response, in terms of its spatial distribution, its lagged nature and its intraseasonal evolution, can be explained primarily by the superposition of SC signals in the early-winter NAO response and the late-winter EA response. The sum of these NAO and EA contributions explains almost 80% of the total DJF mslp anomalies at lag +3 years seen in Figure 2.

The origin of the SC signal in the EA pattern is not clear and deserves further investigation. There are a number of potential interactions and influences that

deserve consideration, including those associated with the well-known (bottom-up) SC surface responses in the Pacific. For example, in years following S_{max}, Misios *et al.* (2019) identified increased rainfall in the equatorial Pacific, an eastward shift of the Walker circulation and positive sea surface temperature anomalies in the equatorial Pacific resembling observed changes during El Nino events, albeit of considerably weaker magnitude. It would be interesting to investigate whether this response could propagate to the NA and project onto the EA pattern, as identified in typical El Nino years (Ayarzagüena *et al.*, 2018) although this is beyond the scope of this study. Previous studies have suggested that a late-winter EA response might be traced to stratospheric pathways whereas teleconnections mediated via the troposphere are more likely to impact the early-winter EA pattern (e.g., King *et al.*, 2018). Our analysis identifies the strongest positive EA response in late winter, hinting at a possible stratospheric pathway.

Interestingly, our result showing an 11-year SC in the EA pattern is similar to the results of Sjolte *et al.* (2018). They developed a reconstruction of atmospheric winter circulation for the NA region covering the period 1241–1970 CE based on seasonally resolved Greenland ice core records and a 1200-year-long simulation with an isotope-enabled climate model. The mslp and surface temperature were reconstructed by matching the spatiotemporal variability in the modelled isotopic composition to that of the ice cores. Previous paleoclimate studies have indicated solar influences on climate in the NA region on centennial timescales (Adolphi *et al.*, 2014; Bond *et al.*, 2001; Jiang *et al.*, 2015), including a link between climate conditions during the Little Ice Age and a negative NAO forced by low solar activity (Shindell *et al.*, 2001; Swingedouw *et al.*, 2017). However, Sjolte *et al.* (2018) found no persistent relationship between solar forcing and the NAO. Instead, they found a strong impact of solar forcing on the secondary mode of circulation represented by EOF-2 of their reconstructed mslp, that is, the EA pattern. The strongest correspondence occurred at five-year lags which they suggested was indicative of an atmosphere–ocean feedback. They proposed a possible mechanism that involved an increase in atmospheric blocking (Woollings *et al.*, 2010) and weakening of the subpolar gyre (Huo *et al.*, 2024; Moffa-Sánchez & Hall, 2017). This mechanism also warrants further investigation using more comprehensive reanalysis datasets. The 20CRv3 reanalysis dataset employed in this study was created as a coupled ocean–atmosphere reanalysis so there is also a physically consistent companion oceanic dataset that should allow further exploration of these possible 'bottom-up' mechanisms (outside the scope of the current study).

In summary, a detailed decomposition of the observed wintertime mslp response to 11-year solar forcing between the primary modes of variability (the NAO and EA pattern) and between the early and late winter responses has provided an improved understanding of the interplay between the leading modes of variability in shaping the overall mslp response. However, while the study identifies significant solar signals in both EA and NAO patterns, the physical mechanisms driving these responses remain inadequately elucidated. The origin of the previously unidentified delayed response in the EA pattern warrants further examination. We also note that the results are derived from a MLR analysis which has limitations, including its assumption of linearity, stationarity and dependence on the choice of predictors. There is always the chance that an internal mode of the atmosphere–ocean coupled system could, by chance, align and be mistaken for a SC signal, especially since the observational record is relatively short.

ACKNOWLEDGEMENTS

The authors thank the three reviewers for their valuable comments that have improved the paper. The publication of this article in OA mode was financially supported by HEAL-Link.

FUNDING INFORMATION

Paula L. M. Gonzalez, Lesley J. Gray and Scott Osprey were funded by the UK Natural Environment Research Council (NERC) North Atlantic Climate System Integrated Study (ACSIS; grant no. NE/V013130/1), CANARI programme, and the National Centre for Atmospheric Science (NCAS). Paula L. M. Gonzalez was also funded by the NCAS National Capability Programme ACREW (grant no. NE/R000034/1) funded by NERC and GCRF. Stergios Misios is funded by the Hellenic Foundation for Research and Innovation (Project Acronym: StratoFIRE, Project: grant no. 3995).

CONFLICT OF INTEREST STATEMENT

No conflict of interest is declared.

DATA AVAILABILITY STATEMENT

ERA5 reanalysis data used in this study are freely available from the Copernicus Climate Change Service (C3S) Climate Data Store (https://cds.climate.copernicus.eu). The NOAA-CIRES-DOE 20th Century Reanalysis version 3 (20CRv3) dataset is publicly available at https://psl.noaa.gov/data/20thC_Rean/. The code for the EOF analysis and the figures is available on https://github.com/smisios/misios2025. The Butterworth filter is implemented in scipy.*signal* by specifying order 6 and high-pass cut-off period 18 years. The code is available on github.

ORCID

Stergios Misios https://orcid.org/0000-0003-1226-4719
Paula L. M. Gonzalez https://orcid.org/0000-0003-0154-0087

REFERENCES

Adolphi, F., Muscheler, R., Svensson, A., Aldahan, A., Possnert, G., Beer, J. et al. (2014) Persistent link between solar activity and Greenland climate during the last glacial maximum. *Nature Geoscience*, 7, 662–666.

Allan, R. & Ansell, T. (2006) A new globally complete monthly historical gridded mean sea level pressure dataset (HadSLP2): 1850-2004. *Journal of Climate*, 19, 5816–5842.

Andrews, M.B., Knight, J.R. & Gray, L.J. (2015) A simulated lagged response of the North Atlantic oscillation to the solar cycle over the period 1960–2009. *Environmental Research Letters*, 10, 054022.

Anstey, J.A., Simpson, I.R., Richter, J.H., Naoe, H., Taguchi, M., Serva, F. et al. (2022) Teleconnections of the quasi-biennial oscillation in a multi-model ensemble of QBO-resolving models. *Quarterly Journal of the Royal Meteorological Society*, 148, 1568–1592.

Ayarzagüena, B., Ineson, S., Dunstone, N.J., Baldwin, M.P. & Scaife, A.A. (2018) Intraseasonal effects of El Niño–southern oscillation on North Atlantic climate. *Journal of Climate*, 31, 8861–8873.

Baldwin, M.P. & Dunkerton, T.J. (2001) Stratospheric harbingers of anomalous weather regimes. *Science*, 294, 581–584.

Barnes, E.A. & Polvani, L.M. (2015) CMIP5 projections of Arctic amplification, of the north American/North Atlantic circulation, and of their relationship. *Journal of Climate*, 28, 5254–5271.

Bellouin, N., Quaas, J., Gryspeerdt, E., Kinne, S., Stier, P., Watson-Parris, D. et al. (2020) Bounding global aerosol radiative forcing of climate change. *Reviews of Geophysics*, 58, e2019RG000660.

Bond, G., Kromer, B., Beer, J., Muscheler, R., Evans, M.N., Showers, W. et al. (2001) Persistent solar influence on North Atlantic climate during the Holocene. *Science*, 294, 2130–2136.

Cassou, C., Terray, L., Hurrell, J.W. & Deser, C. (2004) North Atlantic winter climate regimes: spatial asymmetry, stationarity with time, and oceanic forcing. *Journal of Climate*, 17, 1055–1068.

Chiodo, G., Calvo, N., Marsh, D.R. & Garcia-Herrera, R. (2012) The 11 year solar cycle signal in transient simulations from the whole atmosphere community climate model. *Journal of Geophysical Research-Atmospheres*, 117, 1–21.

Chiodo, G., Oehrlein, J., Polvani, L.M., Fyfe, J.C. & Smith, A.K. (2019) Insignificant influence of the 11-year solar cycle on the North Atlantic oscillation. *Nature Geoscience*, 12, 94–99.

Dimdore-Miles, O., Gray, L. & Osprey, S. (2021) Origins of multi-decadal variability in sudden stratospheric warmings. *Weather and Climate Dynamics*, 2, 205–231.

Drews, A., Huo, W., Matthes, K., Kodera, K. & Kruschke, T. (2022) The Sun's role in decadal climate predictability in the North Atlantic. *Atmospheric Chemistry and Physics*, 22, 7893–7904.

Frame, T.H.A. & Gray, L.J. (2010) The 11-Yr solar cycle in ERA-40 data: an update to 2008. *Journal of Climate*, 23, 2213–2222.

Fujiwara, M., Wright, J.S., Manney, G.L., Gray, L.J., Anstey, J., Birner, T. et al. (2017) Introduction to the SPARC reanalysis Intercomparison project (S-RIP) and overview of the reanalysis systems. *Atmospheric Chemistry and Physics*, 17, 1417–1452.

García-Franco, J.L., Gray, L.J., Osprey, S., Chadwick, R. & Martin, Z. (2022) The tropical route of quasi-biennial oscillation (QBO) teleconnections in a climate model. *Weather and Climate Dynamics*, 3, 825–844.

Gray, L., Beer, J., Geller, M., Haigh, J.D., Lockwood, M., Matthes, K. et al. (2010) Solar influences on climate. *Reviews of Geophysics*, 48, RG4001.

Gray, L., Scaife, A.A., Mitchell, D.M., Osprey, S., Ineson, S., Hardiman, S. et al. (2013) A lagged response to the 11 year solar cycle in observed winter Atlantic/European weather patterns. *Journal of Geophysical Research: Atmospheres*, 118(24), 13–405.

Gray, L.J., Woollings, T.J., Andrews, M. & Knight, J. (2016) Eleven-year solar cycle signal in the NAO and Atlantic/European blocking. *Quarterly Journal of the Royal Meteorological Society*, 142, 1890–1903.

Haigh, J.D. (2001) Climate - climate variability and the influence of the sun. *Science*, 294, 2109–2111.

Haigh, J.D. & Blackburn, M. (2006) Solar influences on dynamical coupling between the stratosphere and troposphere. *Space Science Reviews*, 125, 331–344.

Hall, R.J. & Hanna, E. (2018) North Atlantic circulation indices: links with summer and winter UK temperature and precipitation and implications for seasonal forecasting. *International Journal of Climatology*, 38, e660–e677.

Hersbach, H., Bell, B., Berrisford, P., Hirahara, S., Horányi, A., Muñoz-Sabater, J. et al. (2020) The ERA5 global reanalysis. *Quarterly Journal of the Royal Meteorological Society*, 146, 1999–2049.

Holton, J.R. & Tan, H.-C. (1980) The influence of the equatorial quasi-biennial oscillation on the global circulation at 50 mb. *Journal of Atmospheric Sciences*, 37, 2200–2208.

Hood, L.L. & Soukharev, B.E. (2012) The lower-stratospheric response to 11-Yr solar forcing: coupling to the Troposphere–Ocean response. *Journal of the Atmospheric Sciences*, 69, 1841–1864.

Huo, W., Drews, A., Martin, T. & Wahl, S. (2024) Impacts of North Atlantic model biases on natural decadal climate variability. *Journal of Geophysical Research: Atmospheres*, 129, e2023JD039778.

Hurrell, J.W., Kushnir, Y., Ottersen, G. & Visbeck, M. (2003) An overview of the North Atlantic oscillation. In: *The North Atlantic oscillation: climatic significance and environmental impact*. Washington: American Geophysical Union.

Hurrell, J.W. & van Loon, H. (1997) Decadal variations in climate associated with the NORTH ATLANTIC oscillation. *Climatic Change*, 36, 301–326.

Ineson, S., Scaife, A.A., Knight, J.R., Manners, J.C., Dunstone, N.J., Gray, L.J. et al. (2011) Solar forcing of winter climate variability in the northern hemisphere. *Nature Geoscience*, 4, 753–757.

James, I.N. & James, P.M. (1989) Ultra-low-frequency variability in a simple atmospheric circulation model. *Nature*, 342, 53–55.

Jiang, H., Muscheler, R., BJörck, S., Seidenkrantz, M.-S., Olsen, J., Sha, L. et al. (2015) Solar forcing of Holocene summer sea-surface temperatures in the northern North Atlantic. *Geology*, 43, 203–206.

Jones, P.D., Jonsson, T. & Wheeler, D. (1997) Extension to the North Atlantic oscillation using early instrumental pressure observations from Gibraltar and south-west Iceland. *International Journal of Climatology*, 17, 1433–1450.

King, M.P., Herceg-Bulić, I., Bladé, I., García-Serrano, J., Keenlyside, N., Kucharski, F. et al. (2018) Importance of late fall ENSO teleconnection in the euro-Atlantic sector. *Bulletin of the American Meteorological Society*, 99, 1337–1343.

Klavans, J.M., Clement, A.C., Cane, M.A. & Murphy, L.N. (2022) The evolving role of external forcing in North Atlantic SST variability over the last millennium. *Journal of Climate*, 35, 2741–2754.

Kodera, K. & Kuroda, Y. (2002) Dynamical response to the solar cycle. *Journal of Geophysical Research-Atmospheres*, 107, 4749.

Kuchar, A., Ball, W.T., Rozanov, E.V., Stenke, A., Revell, L., Miksovsky, J. et al. (2017) On the aliasing of the solar cycle in the lower stratospheric tropical temperature. *Journal of Geophysical Research: Atmospheres*, 122, 9076–9093.

Kuroda, Y., Kodera, K., Yoshida, K., Yukimoto, S. & Gray, L. (2022) Influence of the solar cycle on the North Atlantic oscillation. *Journal of Geophysical Research: Atmospheres*, 127, e2021JD035519.

Labitzke, K. & van Loon, H. (2000) The QBO effect on the solar signal in the global stratosphere in the winter of the northern hemisphere. *Journal of Atmospheric and Solar-Terrestrial Physics*, 62, 621–628.

Lean, J. & Rind, D.H. (2008) How natural and anthropogenic influences alter global and regional surface temperatures: 1889 to 2006. *Geophysical Research Letters*, 35, L18701.

Lean, J.L. & Rind, D.H. (2009) How will Earth's surface temperature change in future decades? *Geophysical Research Letters*, 36, L15708.

Lockwood, M., Harrison, R.G., Woollings, T. & Solanki, S.K. (2010) Are cold winters in Europe associated with low solar activity? *Environmental Research Letters*, 5, 024001.

Ma, H., Haishan, C., Lesley, G., Liming, Z., Xing, L., Ruili, W. et al. (2018) Changing response of the North Atlantic/European winter climate to the 11 year solar cycle. *Environmental Research Letters*, 13, 034007.

Maliniemi, V., Asikainen, T., Salminen, A. & Mursula, K. (2019) Assessing North Atlantic winter climate response to geomagnetic activity and solar irradiance variability. *Quarterly Journal of the Royal Meteorological Society*, 145, 3780–3789.

Meehl, G.A., Arblaster, J.M., Matthes, K., Sassi, F. & van Loon, H. (2009) Amplifying the Pacific climate system response to a small 11-year solar cycle forcing. *Science*, 325, 1114–1118.

Misios, S., Gray, L.J., Knudsen, M.F., Karoff, C., Schmidt, H. & Haigh, J. (2019) Slowdown of the Walker circulation at solar cycle maximum. PNAS. *Slowdown of the Walker Circulation at Solar Cycle Maximum*, 116, 7186–7191.

Misios, S., Mitchell, D.M., Gray, L.J., Tourpali, K., Matthes, K., Hood, L. et al. (2016) Solar signals in CMIP-5 simulations: effects of Atmosphere-Ocean coupling. *Quarterly Journal of the Royal Meteorological Society*, 142, 928–941.

Misios, S. & Schmidt, H. (2012) Mechanisms involved in the amplification of the 11-yr solar cycle signal in the tropical Pacific Ocean. *Journal of Climate*, 25, 5102–5118.

Misios, S. & Schmidt, H. (2013) The role of the oceans in shaping the tropospheric response to the 11 year solar cycle. *Geophysical Research Letters*, 40, 6377.

Moffa-Sánchez, P. & Hall, I.R. (2017) North Atlantic variability and its links to European climate over the last 3000 years. *Nature Communications*, 8, 1726.

Ottera, O.H., Bentsen, M., Drange, H. & Suo, L.L. (2010) External forcing as a metronome for Atlantic multidecadal variability. *Nature Geoscience*, 3, 688–694.

Roy, I. & Haigh, J.D. (2010) Solar cycle signals in sea level pressure and sea surface temperature. *Atmospheric Chemistry and Physics*, 10, 3147–3153.

Sato, M., Hansen, J.E., Mccormick, M.P. & Pollack, J.B. (1993) Stratospheric aerosol optical depths, 1850-1990. *Journal of Geophysical Research-Atmospheres*, 98, 22987–22994.

Scaife, A.A., Comer, R.E., Dunstone, N.J., Knight, J.R., Smith, D.M., Maclachlan, C. et al. (2017) Tropical rainfall, Rossby waves and regional winter climate predictions. *Quarterly Journal of the Royal Meteorological Society*, 143, 1–11.

Scaife, A.A., Ineson, S., Knight, J.R., Gray, L., Kodera, K. & Smith, D.M. (2013) A mechanism for lagged North Atlantic climate response to solar variability. *Geophysical Research Letters*, 40, 439.

Scaife, A.A. & Smith, D. (2018) A signal-to-noise paradox in climate science. *npj Climate and Atmospheric Science*, 1, 28.

Seppälä, A. & Clilverd, M.A. (2014) Energetic particle forcing of the northern hemisphere winter stratosphere: comparison to solar irradiance forcing. *Frontiers in Physics*, 2, 25.

Shindell, D.T., Schmidt, G.A., Mann, M.E., Rind, D. & Waple, A. (2001) Solar forcing of regional climate change during the maunder minimum. *Science*, 294, 2149–2152.

Sjolte, J., Sturm, C., Adolphi, F., Vinther, B.M., Werner, M., Lohmann, G. et al. (2018) Solar and volcanic forcing of North Atlantic climate inferred from a process-based reconstruction. *Climate of the Past*, 14, 1179–1194.

Slivinski, L.C., Compo, G.P., Whitaker, J.S., Sardeshmukh, P.D., Giese, B.S., Mccoll, C. et al. (2019) Towards a more reliable historical reanalysis: improvements for version 3 of the twentieth century reanalysis system. *Quarterly Journal of the Royal Meteorological Society*, 145, 2876–2908.

Spiegl, T.C., Langematz, U., Pohlmann, H. & KRöger, J. (2023) A critical evaluation of decadal solar cycle imprints in the MiKlip historical ensemble simulations. *Weather and Climate Dynamics*, 4, 789–807.

Swingedouw, D., Mignot, J., Ortega, P., Khodri, M., Menegoz, M., Cassou, C. et al. (2017) Impact of explosive volcanic eruptions on the main climate variability modes. *Global and Planetary Change*, 150, 24–45.

Thieblemont, R., Matthes, K., Omrani, N.-E., Kodera, K. & Hansen, F. (2015) Solar forcing synchronizes decadal North Atlantic climate variability. *Nature Communications*, 6, 8268.

Tung, K.K. & Zhou, J.S. (2010) The Pacific's response to surface heating in 130 Yr of SST: La Nina-like or El Nino-like? *Journal of the Atmospheric Sciences*, 67, 2649–2657.

Wallace, J.M. & Gutzler, D.S. (1981) Teleconnections in the geopotential height field during the northern hemisphere winter. *Monthly Weather Review*, 109, 784–812.

White, W., Lean, J., Cayan, D.R. & Dettinger, M.D. (1997) Response of global upper ocean temperature to changing

solar irradiance. *Journal of Geophysical Research-Oceans*, 102, 3255–3266.

White, W.B., Dettinger, M.D. & Cayan, D.R. (2003) Sources of global warming of the upper ocean on decadal period scales. *Journal of Geophysical Research-Oceans*, 108, 3248.

Woollings, T., Lockwood, M., Masato, G., Bell, C. & Gray, L. (2010) Enhanced signature of solar variability in Eurasian winter climate. *Geophysical Research Letters*, 37, 1–6.

Zhao, L., Wang, J., Xiao, Z., Ding, Y., Huo, W. & Liu, J. (2025) Solar 11-year cycle-modulated north–south contrasting patterns of summer precipitation in China. *Journal of Climate*, 38, 3277–3294.

How to cite this article: Misios, S., Gonzalez, P.L.M., Gray, L.J., Osprey, S. & Ma, H. (2026) Diagnosing the 11-year solar cycle's influence on the East Atlantic pattern. *Quarterly Journal of the Royal Meteorological Society*, e70187. Available from: https://doi.org/10.1002/qj.70187